Journal of Solid State Chemistry 215 (2014) 292–299

Contents lists available at ScienceDirect

Journal of Solid State Chemistry

journal homepage: www.elsevier.com/locate/jssc

# Copper(II) complexes with 4-(1*H*-1, 2, 4-trizol-1-ylmethyl) benzoic acid: Syntheses, crystal structures and antifungal activities

Pingping Xiong [a,1], Jie Li [b,1], Huaiyu Bu [b,*], Qing Wei [a], Ruolin Zhang [b], Sanping Chen [a,**]

[a] Key Laboratory of Synthetic and Natural Functional Molecule Chemistry of Ministry of Education, College of Chemistry and Materials Science, Northwest University, Xi'an 710069, China

[b] Key Laboratory of Resource Biology and Biotechnology in Western China (Ministry of Education), Shaanxi Provincial Key Laboratory of Biotechnology, Xi'an 710069, China

ARTICLE INFO

*Article history:*
Received 22 December 2013
Received in revised form
7 April 2014
Accepted 20 April 2014
Available online 29 April 2014

*Keywords:*
Copper(II) compound
4-(1*H*-1, 2, 4-trizol-1-ylmethyl) benzoic acid
Crystal structure
Antifungal activity

ABSTRACT

Reaction of Cu(II) with an asymmetric semi-rigid organic ligand 4-(1*H*-1, 2, 4-trizol-1-ylmethyl) benzoic acid (HL), yielded five compounds, **$[Cu_{0.5}L]_n$** (**1**), **$[Cu(HL)_2Cl_2]_n$** (**2**), **$[Cu(HL)_2Cl_2(H_2O)]$** (**3**), **$[Cu(L)_2(H_2O)]_n$** (**4**) and **$[Cu(L)(phen)(HCO_2)]_n$** (**5**), which have been fully characterized by infrared spectroscopy, elemental analysis, and single-crystal X-ray diffraction. As for compounds **1**, **2** and **5**, Cu(II) is bridged through HL, $Cl^-$, and formic acid, respectively, featuring 1D chain-structure. In compound **3**, Cu(II) with hexahedral coordination sphere is assembled through hydrogen-bonding into 3D supramolecular framework. In compound **4**, 1D chain units –Cu–O–Cu–O– are ligand-bridged into a 3D network. All compounds were tested on fungi (*Fusarium graminearum*, *Altemaria solani*, *Macrophoma kawatsukai*, *Alternaria alternata* and *Colletotrichum gloeosporioides*). Compound **1** exhibits a better antifungal effect compared to other compounds. An effect of structure on the antifungal activity has also been correlated.



## 1. Introduction

1*H*-1, 2, 4-triazole derivatives as a broad-spectrum, highly effective antifungal fungicide, has been much concerned [1]. Remarkably, triazoles inhibit sterol 14R-demethylase, thus interfere with fungal cell-wall formation [2]. Its outstanding pesticide effect contributes to the development prospect of triazole-based compounds [1]. So far, the pesticides on market are mainly composed of these triazole fungicides, such as difenoconazole, diniconazole, tebuconazole, flutriafol, hexaconazole and cyproconazole [3–7].

Compared to conventional triazole fungicides, the metal coordination compounds pesticides could be utilized as a kind of controlled release formulations which has the capacity of alleviating the toxicity and decreasing the pesticide residue [8]. In addition to the excellent characteristics of the original, the new pesticide metal coordination compounds also have the advantages of increasing efficacy, even the stability of the original drug, reducing pesticide dosage, as well as other biological functions [9–11]. The modification in structure of triazole can influence the antifungal activity, expand the bactericidal spectrum and renovate the issue about resistance of sterilization [12]. To explore a new metal coordination compound pesticide has a profound potential of development and utilization in agricultures [13].

In this paper, we selected the 4-(1*H*-1, 2, 4-trizol-1-ylmethyl) benzoic acid as the ligand, where oxygen atoms in the carboxylic group and N atoms from the triazole ring both are apt to coordinate with Cu ions. As well-known, the coordination modes of the carboxyl oxygen can be roughly summarized as monodentate-coordinated, chelating-coordinated and bridging-coordinated [14,15]. Based on flexible coordination modes of carboxylic group and antifungal activity of trizole molecule, five copper(II) coordination compounds were synthesized and structurally characterized. Antifungal tests showed that compound **1** exhibited the best antifungal activity.

## 2. Experimental

### 2.1. Materials and methods

Elemental analyses were performed on an Elementar Vario EL III analyzer. IR spectra were recorded on a Tensor 27 spectrometer (Bruker Optics, Ettlingen, Germany) as KBr pellets in the range of 4000–400 $cm^{-1}$. Powder X-ray diffraction (PXRD) patterns were obtained on a Bruker D8 ADVANCE X-ray powder diffractometer

* Corresponding author.
** Corresponding author. Tel./fax: +86 2988302604.
*E-mail addresses:* 7213792@qq.com (H. Bu), sanpingchen@126.com, sanpingchen312@gmail.com (S. Chen).
[1] These authors contributed equally to this work.

http://dx.doi.org/10.1016/j.jssc.2014.04.012
0022-4596/

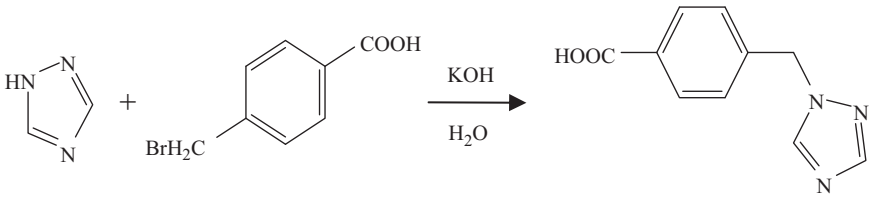


**Scheme 1.** Synthesis of the ligand.

with Cu *K*α radiation ($\lambda$=1.5405 Å). Thermogravimetric measurements were carried out from room temperature to 1000 °C for **1**–**5** in simulated nitrogen atmosphere using a NETRZSCH STA 449C equipment with a heating rate of 10 °C $min^{-1}$.

### 2.2. Synthesis

#### 2.2.1. Preparation of 4-(1H-1, 2, 4-trizol-1-ylmethyl) benzoic acid (*HL*)

The ligand was synthesized using a literature procedure (Scheme 1) [16,17]. IR (KBr pellet, $cm^{-1}$) for **HL**: 3453, 3119, 2952, 2363, 1914, 1694, 1515, 1433, 1275, 1141, 1011, 919, 731, and 677. m. p 215.1–215.5 °C.

#### 2.2.2. Preparation of $[Cu_{0.5}L]_n$ (*1*)

A mixture of HL (20.3 mg, 0.10 mmol) and $CuCl_2 \cdot 2H_2O$ (17.0 mg, 0.10 mmol) was dissolved in distilled $H_2O$ (3 mL), which were sealed in a 10 mL Teflon-lined stainless steel autoclave. The mixture was heated at 140 °C for 72 h, cooled to 100 °C at a rate of 5 °C $h^{-1}$, and held at this temperature for 10 h. Then, it was cooled to room temperature at a rate of 5 °C $h^{-1}$. Purple lump crystals were isolated in 45% yield (based on HL). $^1$H NMR (400 MHz, DMSO-$d_6$): $\delta$ 8.650 (*s*, 1H, CH), 8.004 (*s*, 1H, CH), 7.933 (*d*, 2H, *p*-$C_6H_4$), 7.331 (*d*, 2H, *p*-$C_6H_4$), 5.540 (*s*, 2H, $CH_2$). IR (KBr pellet, $cm^{-1}$): 3455 (b), 1608 (*s*), 1562 (m), 1371 (*s*), 1288 (m), 1119 (m), 736 (m), 674 (m) (Fig. S1). Elemental analysis calculated for $C_{20}H_{16}CuN_6O_4$: C 51.29%, H 3.41%, N 17.95%; found: C 51.11%, H 3.74%, N 17.80%.

#### 2.2.3. Preparation of $[Cu(HL)_2Cl_2]_n$ (*2*)

Compound **2** was synthesized by the identical pathway with compound **1**. In the above method, the purple lump crystals (**1**) can be obtained while a small amount of blue–green block crystals (**2**) can be received at the same time. In order to improve the yield of compound **2**, the temperature was increased to 160 or 180 °C, then almost only compound **2** left. Since the color and the shape are different for each other, we simply separate them by hands. Blue–green block crystals were isolated in 65% yield (based on HL). $^1$H NMR (400 MHz, DMSO-$d_6$): $\delta$ 13.083 (*s*, 1H, COOH), 8.737 (*s*, 1H, CH), 8.183 (*s*, 1H, CH), 7.926 (*d*, 2H, *p*-$C_6H_4$), 7.309 (*d*, 2H, *p*-$C_6H_4$), 5.723 (*s*, 2H, $CH_2$). IR (KBr pellet, $cm^{-1}$): 3444(b), 1616(s), 1564(s), 1374(s), 1279(m), 1123(m), 1001(m), 768(m), 742(s), 673(m) (Fig. S1). Elemental analysis calculated for $C_{20}H_{18}Cl_2CuN_6O_4$: C 44.38%, H 3.33%, N 15.53%; found: C 44.25%, H 3.63%, N 15.36%.

#### 2.2.4. Preparation of $[Cu(HL)_2Cl_2(H_2O)]$(*3*)

Different with **1** and **2**, compound **3** was obtained from mother liquor of the hydrothermal reaction above. The temperature region of the hydrothermal reaction must be in the range from 140–180 °C. Upon being disturbed for four weeks, blue strip crystals were isolated in 10% yield (based on HL). $^1$H NMR (400 MHz, DMSO-$d_6$): $\delta$ 13.194 (*s*, 1H, COOH), 8.949 (*s*, 1H, CH), 8.294 (*s*, 1H, CH), 7.926 (*d*, 2H, *p*-$C_6H_4$), 7.303 (*d*, 2H, *p*-$C_6H_4$), 5.818 (*s*, 2H, $CH_2$). IR (KBr pellet, $cm^{-1}$): 3446 (b), 1674 (s), 1610 (m), 1429 (s), 1323 (s), 1293 (s), 1183 (m), 1127 (s), 995 (m), 742 (s), 669 (m) (Fig. S1). Elemental analysis calculated for $C_{20}H_{20}Cl_2CuN_6O_5$: C 42.94%, H 3.58%, N 15.03%; found: C 43.15%, H 3.45%, N 14.95%.

#### 2.2.5. Preparation of $[Cu(L)_2(H_2O)]_n$ (*4*)

Just like the compounds **1** and **2**, compound **4** was obtained in the same way. At 140 °C, the yield of compound **4** and the crystal shape are much better. Blue lump crystals were isolated by hands in 15% yield (based on HL). $^1$H NMR (400 MHz, DMSO-$d_6$): $\delta$ 8.925 (*s*, 1H, CH), 8.315 (*s*, 1H, CH), 7.954 (*d*, 2H, *p*-$C_6H_4$), 7.364 (*d*, 2H, *p*-$C_6H_4$), 5.818 (*s*, 2H, $CH_2$). IR (KBr pellet, $cm^{-1}$): 3455(b), 1633(s), 1556(w), 1382(m), 1287(w), 1131(w), 1019(w), 759(m), 673(w) (Fig. S1). Elemental analysis calculated for $C_{20}H_{18}CuN_6O_5$: C 49.39%, H 3.70%, N 17.29%; found: C 49.22%, H 3.99%, N 17.17%.

#### 2.2.6. Preparation of $[Cu(L)(phen)(HCO_2)]_n$ (*5*)

A mixture of HL (20.3 mg, 0.10 mmol), $CuCl_2.2H_2O$ (17.0 mg, 0.10 mmol), l,10-phenanthroline (19.8 mg, 0.10 mmol) and *N*,*N*-dimethylformamide (DMF)/$H_2O$ (2:3, v/v), which were sealed in a 10 mL Teflon-lined stainless steel autoclave. The mixture has been heated at 140 °C for 10 h and cooled to 100 °C at a rate of 5 °C $h^{-1}$. Upon being held at 100 °C for 72 h, the system was cooled to room temperature at a rate of 5 °C $h^{-1}$. The resulting solution was filtered and transfered in the vial for seven days. Blue triangular shape crystals were isolated and washed with EtOH repeatedly. (Yield: 75%, based on HL). $^1$H NMR (400 MHz, DMSO-$d_6$): $\delta$ 9.455(*s*, 1H, –HCO), 8.682 (*s*, 1H, CH), 8.602 (*d*, 2H, –$C_5H_3N$), 8.068 (*d*, 2H, –$C_5H_3N$), 8.024 (*s*, 1H, CH), 7.924 (*d*, 2H, *p*-$C_6H_4$), 7.618 (*d*, 2H, –$C_6H_2$), 7.307 (*t*, 2H, –$C_5H_3N$), 7.286 (*d*, 2H, *p*-$C_6H_4$), 5.018 (*s*, 2H, $CH_2$). IR (KBr pellet, $cm^{-1}$): 3441 (b), 1628 (s), 1594 (s), 1382 (m), 1018 (m), 852 (m), 723 (m), 678 (m) (Fig. S1). Elemental analysis calculated for $C_{23}H_{17}CuN_5O_4$: C 56.22%, H 3.46%, N 14.26%; found: C 56.15%, H 3.60%, N 14.19%.

### 2.3. Single-crystal structure determination

Selected the suitable single crystals of **1**–**5**, then mounted them onto thin glass fibers and performed the single crystals at 20 °C on a Bruker SMART APEX CCD-based diffractometer in air. All structures were solved by direct methods and refined with full-matrix least-squares refinements based on $F^2$ using SHELXS-97 and SHELXL-97 [18]. Crystal data, data collection parameters, and refinements for **1**–**5** are listed in Table 1. The interatomic bond distances and bond angles of **1**–**5** are given in the Suporting information (Tables S1–S5). CCDC numbers: 970263 and 970264 for **1** and **4**, 970266-970268 for **5**, **3** and **2**, respectively.

### 2.4. Antifungal activities tests

The test microorganisms used in this study were *Fusarium graminearum*, *Altemaria solani*, *Macrophoma kawatsukai*, *Alternaria alternata* and *Colletotrichum gloeosporioides*. The antifungal activities of the compounds were determined by the radial growth method (A.MANN 2008) [19]. In this technique, sterilized hot PDA nutrient medium (composition: potato (200 g), dextrose (15 g), agar (18 g) and distilled water 1000 mL) and 4 mm diameter hole

**Table 1**
Crystallographic data for **1**–**5**.

| Empirical formula | $C_{20}H_{16}CuN_6O_4$ **1** | $C_{20}H_{18}Cl_2CuN_6O_4$ **2** | $C_{20}H_{20}Cl_2CuN_6O_5$ **3** | $C_{20}H_{18}CuN_6O_5$ **4** | $C_{23}H_{17}CuN_5O_4$ **5** |
|---|---|---|---|---|---|
| fw | 467.94 | 540.84 | 558.86 | 485.94 | 490.96 |
| Cryst syst | Monoclinic | Triclinic | Monoclinic | Monoclinic | Orthorhombic |
| $a$ (Å) | 5.3239(10) | 7.5930(14) | 17.899(2) | 23.008(2) | 9.7494(18) |
| $b$ (Å) | 16.558(3) | 7.6304(14) | 8.0675(12) | 9.4363(9) | 9.693(2) |
| $c$ (Å) | 10.639(2) | 19.844(4) | 7.8400(11) | 9.5393(9) | 21.815(4) |
| $\alpha$ (°) | 90 | 83.935(3) | 90 | 90 | 90 |
| $\beta$ (°) | 93.435(4) | 81.248(3) | 95.565(2) | 104.9430(10) | 90 |
| $\gamma$ (°) | 90 | 71.401(3) | 90 | 90 | 90 |
| $V$ (Å$^3$) | 936.2(3) | 1075.0(3) | 1126.8(3) | 2001.0(3) | 2061.6(7) |
| Space group | $P2(1)/c$ | $P$-1 | $P2/c$ | $C2/c$ | $Pna2(1)$ |
| $Z$ value | 2 | 2 | 2 | 4 | 4 |
| $F$ calc (g/cm$^3$) | 1.660 | 1.671 | 1.647 | 1.613 | 1.582 |
| $\mu$ (mm$^{-1}$) | 1.211 | 1.307 | 1.253 | 1.140 | 1.103 |
| Temp (K) | 296(2) | 296(2) | 296(2) | 296(2) | 296(2) |
| No. of observations ($I > 3\sigma$) | 1651 | 3786 | 2002 | 1768 | 2960 |
| Final $R^a$ indices [$I > 2\sigma(I)$]: $R$; $R_w$ | 0.0690; 0.1480 | 0.0572; 0.1484 | 0.0290; 0.0551 | 0.0320; 0.0833 | 0.0555; 0.0926 |

$R1 = \sum||Fo| - |Fc||/\sum|Fo|$. $wR2 = \{\sum[w(Fo^2 - Fc^2)^2]/\sum[w(Fo^2)^2]\}^{1/2}$.

punch were used. Five final concentration solutions in PDA, 0, 30, 60, 90, and 120 μmol/L, were prepared for compound **1**–**5**, **HL**, $CuCl_2$ and l,10-phenanthroline to against *F. graminearum* respectively. Besides that, five final concentration solutions in PDA of compound **1** were used to inhibit the growth of other four fungi (*A. solani*, *M. kawatsukai*, *A. alternata* and *C. gloeosporioides*).

40 mL PDA with each reagent in 50 mL centrifuge tube was divided into three Petri dishes and allowed to solidify. Then the Petri dishes were inculated with 4 mm diameter of the fungi culture by the hole punch. Petri dishes were incubated at 28 °C for 96 h. Antifungal activities were expressed in terms of diameter of growth. All the steps of the above were repeated thrice in our experiment.

## 3. Results and discussion

### 3.1. Temperature effect on the reaction system

In order to explore the temperature effect on the formation of the different compounds from the same system of Cu(II)–4-(1*H*-1, 2, 4-trizol-1-ylmethyl) benzoic acid. As described in preparation of compounds, compounds **1**–**4** were simultaneously generated at 140 °C, like the colored ribbons. Decreasing the temperature down to 120 °C, the final products included a lot of purple crystals and a handful of blue microcrystallines, which were identified to be compounds **1** and **4** by PXRD, respectively (Fig. S2). Further cooling to 90 °C, a great number of purple crystals were structurally characterized as compound **1**, as shown in Fig. S3. That is to say, only one target was obtained. As for the temperatures below 90 °C, there was not any powder or crystalline samples formed except the start materials. It is concluded that, the thermodynamics-controlled temperature regions range from room temperature to 90 °C for **1** and from room temperature to 120 °C for **4**, respectively. The temperature region of 90–120 °C are the kinetics-controlled process for **4**, in which the trace powder samples grow to be crystalline product. According to the above experimental fact, the activation energy of compound **1** is the minimum among the four compounds. With the increase of temperature, the other compounds successively grew, owing to exceeding their activation energy. Accordingly, the reaction is mainly controlled by thermodynamics below 120 °C. Compound **1** is the most thermodynamically stable among these compounds.

Increasing the reaction temperature to 160 °C, the amounts of **1** and **4** markedly drop compared with those at 140 °C, and compound **2** significantly increased and the rest compounds **1** and **4** disappeared. Only compound **2** left at 180 °C (Fig. S4). During the period, the reaction equilibriums of Cu(II) with the ligand shift from one to another with increasing the temperature. As we noticed, the products at higher temperatures are obtained at the expense of those at lower temperatures. In term of thermodynamics stability, compounds **1**–**4** follow the sequence of **1**, **4**, **3** and **2**.

### 3.2. Crystal structure analysis

Among five titled compounds, as shown in Fig. 1, the oxygen atoms of the carboxylic group could coordinate with Cu(II) in terminal monodentate or bidentate, and the N atom from the triazole ring monodentate-bonds with Cu(II).

#### 3.2.1. Structure analysis of compound *1*

In compound **1**, the crystallographically unique copper(II) atom adopts a distorted octahedral coordination sphere, with four carboxylate O atoms from the different carboxylate groups, bidentate coordination in the equatorial plane, and two N donors from triazoles in the axial positions (Fig. 2a).

As shown in Fig. 2b, each copper(II) atom coordinates with four ligands, and each ligand coordinates to two Cu ions. As a bridging ligand, triazole N atoms and carboxylate O atoms are involved in coordination with Cu(II) to form an infinite double Z-shaped 1D chain. In each approximately rectangular ring, the Cu(II)–Cu(II) contact is around 10.639 Å. In parallel with the two 1D chains, the shortest interchain Cu(II)–Cu(II) contact is 5.324 Å.

#### 3.2.2. Structure analysis of compounds *2* and *3*

As shown in Fig. 3a, compound 2 contains two crystallographically independent Cu(II) ions, Cu1 and Cu2, which lie at an inversion center and possess different geometries. Cu1 adopts a distorted octahedral coordination sphere, with four Cl atoms in the equatorial plane, and two N donors from triazoles in the axial positions. Cu2 takes a square-planar environment, with two Cl atoms occupying the equatorial plane, and two N donors from triazoles occupying the axial positions. The adjacent Cu(II) centers are bridged by chloride atoms in μ2-bridging bidentate mode into zigzag 1D infinite chains (Fig. 3b).

In compound **3**, the crystallographically unique copper(II) atom adopts a distorted hexahedral coordination sphere, with two N donors from triazole in the axial positions, one O atom from the

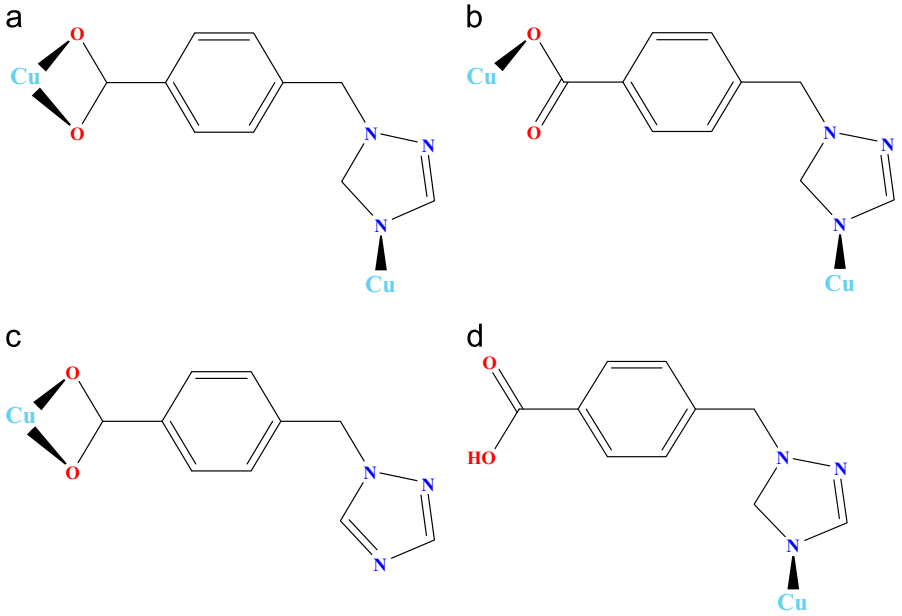


**Fig. 1.** Four kinds of coordination pattern with the metal atoms of the ligand (a–d).

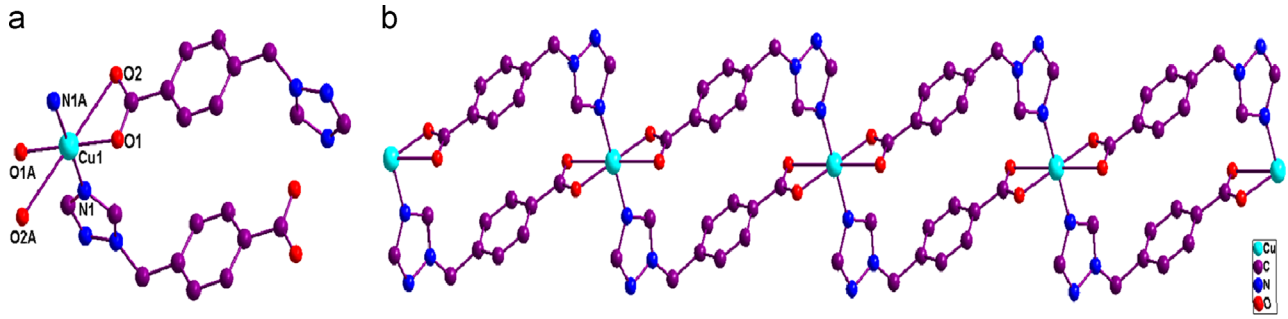


**Fig. 2.** (a) The coordination configuration of **1**. (b) The 1D wavelike chain of **1.**

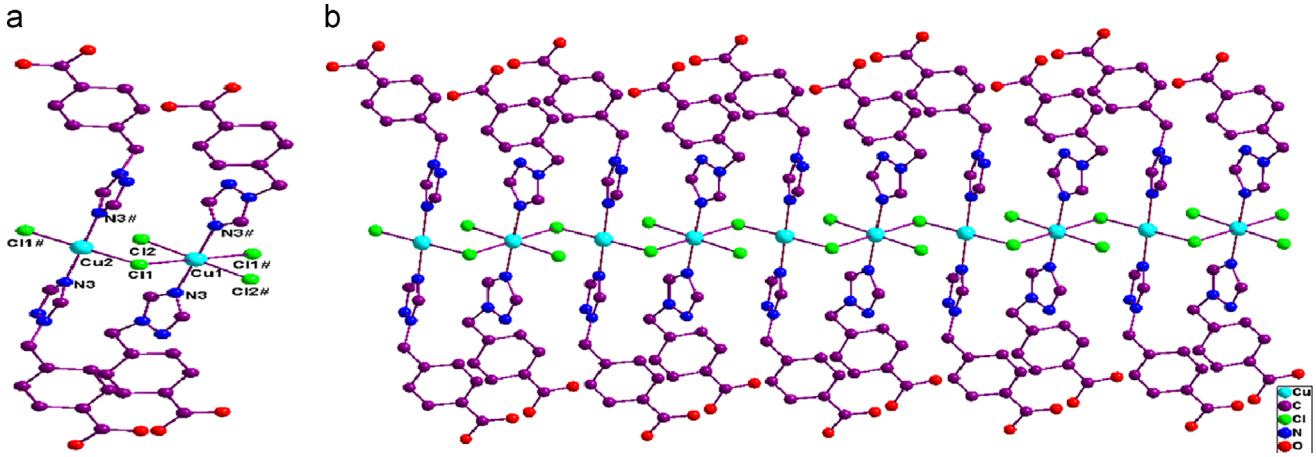


**Fig. 3.** (a) The coordination environment of **2**. (b) The zigzag chain in **2**, the chlorine atoms are regarded as bridging atoms.

water molecules and two Cl atoms coordination in the equatorial plane. The carboxyl oxygen atoms do not participate in coordination, and the compound exists as a separate molecule (Fig. 4a). As presented in Fig. 4b, Cu(II) with hexahedral coordination sphere are assembled through hydrogen-bonding into 3D supramolecule structure.

### 3.2.3. *Structure analysis of compound* ***4***

Compounds **4** and **1** are twin generated. Because of their significantly different colors, it is easy to separate them. In compound **4**, the crystallographically unique copper(II) atom adopts the same coordination configuration as that of compound **1**, with two N atoms donors from triazole, two carboxylate O atoms from the carboxylate

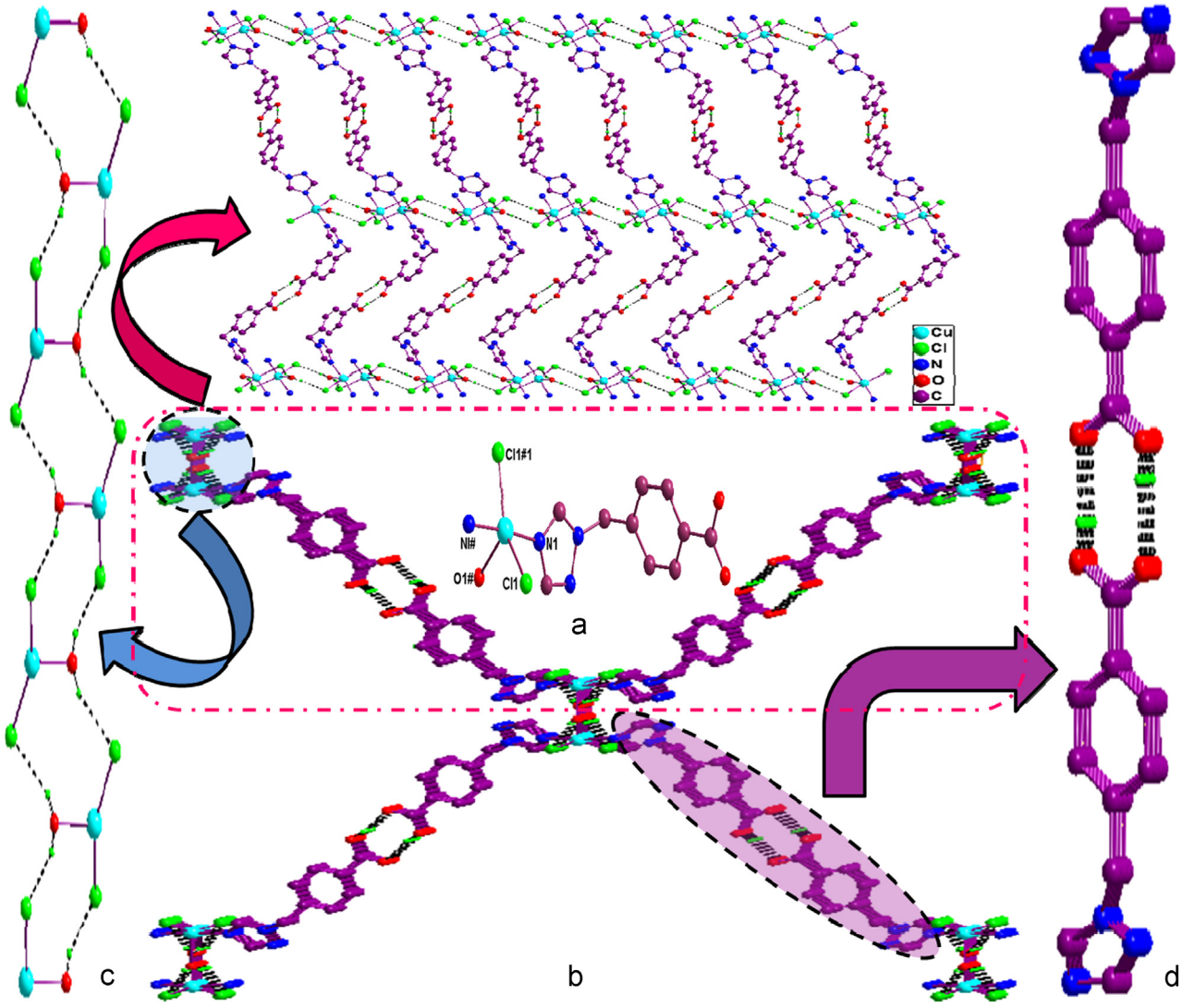


**Fig. 4.** (a) The coordination unit of **3**. (b–d) Two kinds of hydrogen bonds and the 3D structure.

group monodentate coordination in the equatorial plane, and two O atoms from the water molecules coordinated in the axial positions (Fig. 5a). In each distorted rectangular ring, the Cu(II)–Cu(II) bond distance is 12.209 Å, which is longer than that in compound **1**.

In compound **4** (Fig. 5b), O atoms as bridging atom connect with Cu(II), forming an inorganic zigzag chain –Cu–O–Cu–O–. In the 1D zigzag chains, the shortest Cu(II)–Cu(II) bond distance is 4.770 Å. The –Cu–O–Cu–O– 1D zigzag chains are ligand-bridged, leading to a 2D layer. The 2D layers are further ligand-bridged into a 3D network structure.

### 3.2.4. *Structure analysis of compound **5***

In compound **5,** the *N,N*-dimethylformamide (DMF) is hydrolyzed to formic acid molecule. The N atoms from triazole are not involved in coordination. Two N atoms donors from 1,10-phenanthroline and one O atom from the formic acid molecule coordinate to Cu(II) in the equatorial plane. Two carboxylate O atoms in the carboxylate group and one O atom from the formic acid molecule participate in coordination in the axial positions (Fig. 6a).

Compared with compound **2**, compound **5** has a different inorganic zigzag chains –Cu–O–C–O–Cu–O–C–O– and the formic acid molecule are used as a bridging ligand. The copper(II) atoms are linked together through the formic acid molecule with the shortest Cu(II)–Cu(II) bond distance is 5.728 Å (Fig. 6b).

### 3.3. *X-ray powder diffraction and thermal analysis*

As shown in the Supporting information (Fig. S5), X-ray powder diffraction patterns of the samples of **1**–**5** are quite similar to the simulated data of the crystal structure.

To examine the thermal stability of **1**–**5**, the thermogravimetric analyses for crystal samples of **1**–**5** were performed under a simulated nitrogen atmosphere with a heating rate of 10 °C $min^{-1}$ from room temperature up to 1000 °C. The compounds are thermally stable up to 285, 254, 250, 252, and 180 °C for **1**–**5**, respectively. With increasing temperature, the whole frameworks of the compounds collapse (exp. 42.21%, 48.75%, 39.28%, 46.36%, and 33.31% for **1**–**5**). Following that, the intermediates are slowly decomposed, and do not form stable substances until 1000 °C. As shown in Fig. S6, compound **1** shows the highest thermostability, which is consistent with the fact that compound 1 is the most thermodynamically stable among these compounds.

### 3.4. *Antifungal activities of copper(II) compounds*

The primordial data were supposed to be calculated according to the following formulas: 1) Pure increment (mm)=Average diameters of colonies−4 mm diameter of fungal culture; 2) Percentage of antifungal (%)=[(Pure increment of control−Pure increment of treatment)]/Pure increment of control × 100%.

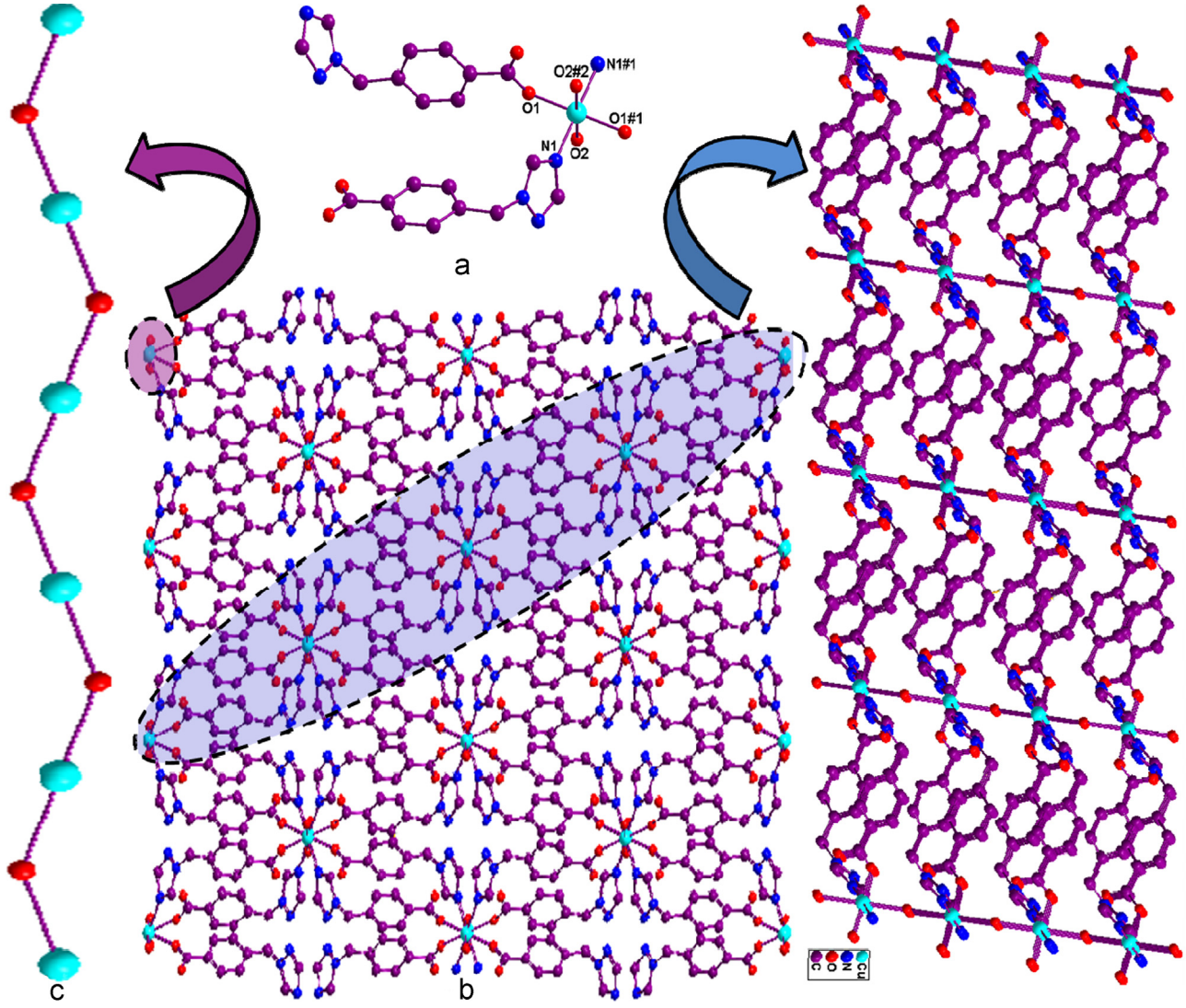


**Fig. 5.** (a) The coordination environment of **4**. (b, c) The inorganic zigzag chains –Cu–O–Cu–O– and the 3D network structure.

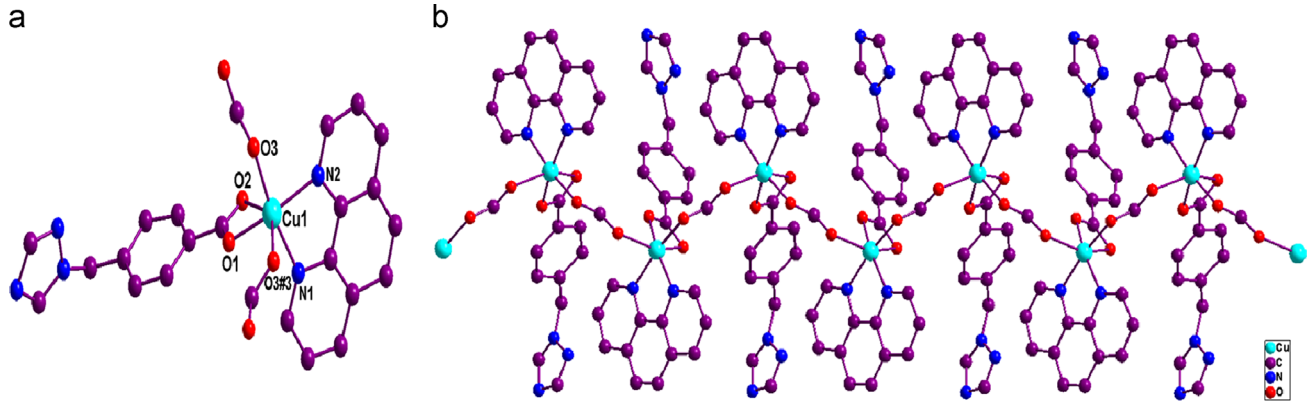


**Fig. 6.** (a) The central atom coordination configuration of **5**. (b) The zigzag chain in (**5**), showing the formic acid molecule bridging of the copper(II) centers.

According to the results and analysis, five compounds show the higher inhibition effect than those of **HL**, $CuCl_2$ and 1,10-phenanthroline (Figs. 7 and S7). For instance, antifungal percentage of compounds **1**–**5** are 72.468%, 63.660%, 68.293%, 70.196%, and 65.796%, respectively. Whereas **HL**, $CuCl_2$ and 1,10-phenanthroline depict antifungal percentage of 61.908%, 24.154%, and 56.337% at 120 μmol/L. It is worth mentioning that **HL**, $CuCl_2$ and 1,10-phenanthroline have a certain degree of antimicrobial effect. However, their antifungal rate are far below the titled copper(II) compounds, especially compound **1** (Table 2).

Among the five novel compounds, compound **1** presents the best antifungal activity compared to compounds **2**–**5**. Visually, diameters of fungal culture under treatment of compound **1** are markedly smaller than those of other groups including **HL** and $CuCl_2$. At the

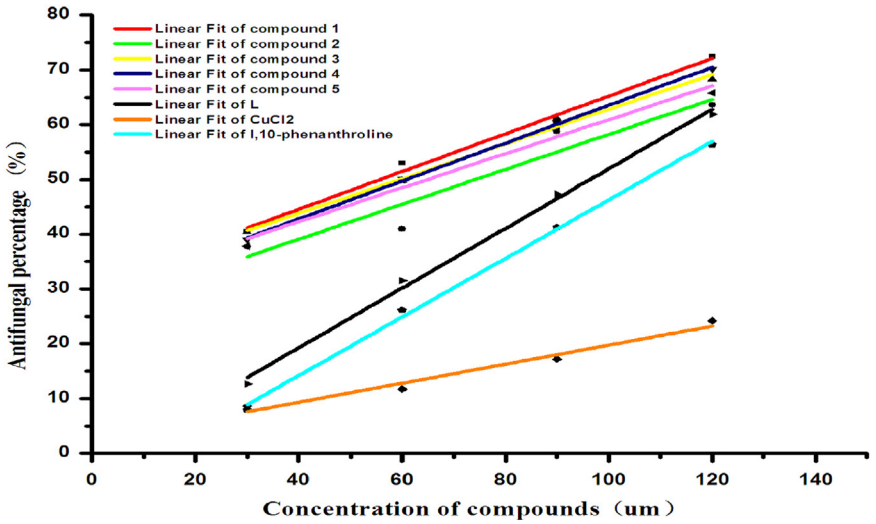


**Fig. 7.** Drug concentration–effect curves of compounds **1**–**5**, **HL**, $CuCl_2$, and l,10-phenanthroline against *Fusarium graminearum*.

**Table 2**
Antifungal activities of compounds **1**–**5**, **HL**, $CuCl_2$, and l,10-phenanthroline against *Fusarium graminearum*.

| Antifungal drugs | Drug concentration–effect curves | *R* | $EC_{50}$ (μmol $L^{-1}$) |
|---|---|---|---|
| Compound **1** | $y=5.0334x-3.509$ | 0.9633 | 49.0343 |
| Compound **2** | $y=4.5483x-3.2612$ | 0.8536 | 65.50885 |
| Compound **3** | $y=4.6459x-2.9746$ | 0.9703 | 85.72352 |
| Compound **4** | $y=5.0522x-3.7133$ | 0.9712 | 53.05178 |
| Compound **5** | $y=4.6284x-3.1176$ | 0.9944 | 56.74139 |
| **L** | $y=8.0151x-10.77$ | 0.9804 | 92.78975 |
| l,10-phenanthroline | $y=7.8479x-11.008$ | 0.9767 | 109.5973 |
| $CuCl_2$ | The inhibition ration of $CuCl_2$ is so low that drug concentration–effect curves is not available | | |

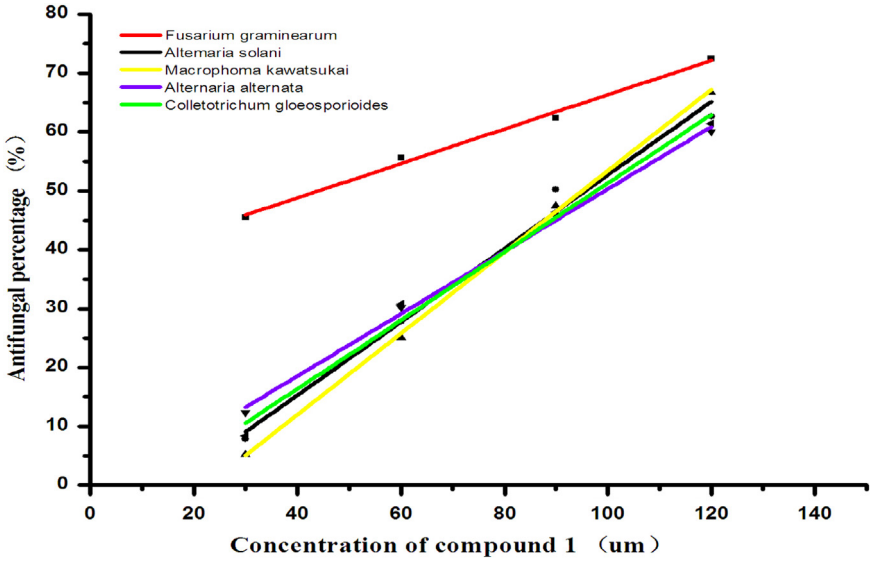


**Fig. 8.** Drug concentration–effect curves of compound **1** against five kinds of fungi.

identical concentration, the antifungal percentage of compound **1** is the highest. The antifungal percentage of the compound **1** ranges from 40.540% to 72.468% with the increase of concentration. The antifungal percentage of compound **2** is the lowest, which varies from 37.721% to 63.660%. And we could draw a conclusion that the antifungal activity of compound **1** is superior to those of the other compounds.

Due to the superiority of compound **1**, we made use of it to test other four fungi (*A. solani*, *M. kawatsukai*, *A. alternata*, and *C. gloeosporioides*) (Fig. S8). All the fungi are retarded by compound **1** to some extent, among which *F. graminearum* shows the highest retardance with an antifungal percentage of 72.468% at 120 μmol/L (Fig. 8 and Table 3).

It is conceivable that ligands contain electron-withdrawing substituents such as −Cl, have greater antifungal activity than electron-donating substituents [20]. Videlicet, the compounds with electron-withdrawing substituents will show a better antifungal activity. However, the chlorine atoms in compounds **2** and **3** lead to only minor increases in the antifungal activities compared to the ligand **HL**. Notably, inhibition percentage of compounds **1**

**Table 3**
Antifungal activity of compound **1** against five kinds of fungi.

| Fungi | Drug concentration–effect curves | *R* | $EC_{50}$ ($\mu$mol $L^{-1}$) |
|---|---|---|---|
| *Fusarium graminearum* | $y=5.0334x-3.509$ | 0.9633 | 49.0343 |
| *Altemaria solani* | $y=9.1983x-13.051$ | 0.9782 | 91.70647 |
| *Macrophoma kawatsukai* | $y=10.034x-14.671$ | 0.9600 | 91.28512 |
| *Alternaria alternata* | $y=7.7721x-10.456$ | 0.9780 | 97.43164 |
| *Colletotrichum gloeosporioides* | $y=8.6322x-12.055$ | 0.9897 | 94.55837 |

and **4** are higher than those of compounds (**2** and **3**) which have electron-withdrawing substituents. Compared to that in the compound **3** (0D, the intramolecular hydrogen bonds assemble the 0D structure into a 3D network structure), the effect of the electron-withdrawing substituents is more significant in compound **2**, which is the reason for compound 2 shows the lowest antifungal activity behavior [3,21–25]. As for compounds **1** and **4**, the complexity and stability of structures probably affect their antifungal activity. Generally speaking, simple structures (compound **1**) have larger possibilities to have good antifungal activity.

## 4. Conclusion

In summary, a family of copper(II) coordination compounds was synthesized and characterized involving 4-(1*H*-1, 2, 4-trizol-1-ylmethyl) benzoic acid. Single-crystal X-ray diffraction analysis revealed that compounds **1**, **2** and **5** all feature a 1D chain, while **3** and **4** exhibit 3D network structure. Antifungal activities analyses show that the title compounds have a higher antifungal activity than those of **HL** and $CuCl_2$. This superiority is probably caused by the special structural features of the coordination compounds. With the combined action between metal ions and ligand, antifungal performances of compounds are greatly improved. Especially for **1,** the inhibition on fungi leads to its protective action on plants probably. A preferable antifungal activity exhibits in **1** by testing against *F. graminearum*. The new Cu-based coordination compound fungicide, is endowed with potent efficacy of antifungal activity. Compound **1** exactly contributes much more than the traditional one to inhibiting fungus. In terms of antifungal we could infer that the fungicide with metal would possess a wider quotation than the traditional one, which inspire us to study the mechanism of crop protection in the next stage.

## Acknowledgments

We gratefully acknowledge the financial support from the National Natural Science Foundation of China (Grant nos. 31201534, 21373162 and 21173168), and the Science Research Projects of Department of Shaanxi Provincial Government (Grant nos. 2010JK882, 2010JQ2007, 11JS110 and 11JK0578).

## Appendix A. Supporting information

Supplementary data associated with this article can be found in the online version at http://dx.doi.org/10.1016/j.jssc.2014.04.012.

## References

[1] O. Prakash, D.K. Aneja, K. Hussain, P. Lohan, P. Ranjan, S. Arora, C. Sharma, K. R. Aneja, Eur. J. Med. Chem. 46 (2011) 5065.
[2] J.J. Manclús, M.J. Moreno, E. Plana, A. Montoya, J. Agric. Food Chem. 56 (2008) 8793.
[3] P.K. Singh, J. Agric. Food Chem. 60 (2012) 5813.
[4] G. Klopman, D. Ptchelintsev, J. Comput. Aided Mol. Des. 7 (1993) 349.
[5] E.M. Ferreira, A.C. Alfenas, L.A. Maffia, R.G. Mafia, A.H. Mounteer, Crop Prot. 27 (2008) 161.
[6] P.A. Worthington, Pestic. Sci. 31 (1991) 457.
[7] S. Reinhard, Zesz. Probl. Postepow Nauk. Rol. 371 (1988) 33.
[8] P.-Z. Zhang, Q.-Y. Fu, R.-X. Chi, C.-X. Yang, J.-G. Xu, J. Zhejiang Univ. Sci. Technol. 15 (2003) 143.
[9] H. Koehle, M.P. Mascianica, A.C. Everson, W02007093535, 2007-08-23.
[10] C.-L. Yang, J.-X. Luo, X.-Q. Xie, Chin. J. Inorg. Chem. 23 (2007) 1259.
[11] R.E. Prasad, M.L. Kantam, B.M. Choudry, Pestic. Sci. 28 (1990) 157.
[12] J.-P. Zhang, X.-M. Chen, J. Am. Chem. Soc. 130 (2008) 6010.
[13] T.P. Murali, E.J. Duncan, Sci. Hortic. 64 (1995) 243.
[14] R.J. Hill, D.L. Long, N.R. Champaness, Acc. Chem. Res. 38 (2005) 337.
[15] B.-H. Ye, M.-L. Tong, X.-M. Chen, Coord. Chem. Rev. 249 (2005) 545.
[16] X.-X. Zhao, J.-P. Ma, Y.-B. Dong, R.-Q. Huang, Cryst. Growth Des. 7 (2007) 1058.
[17] J. Qin, J.-P. Ma, L.-L. Liu, R.-Q. Huang, Y.-B. Dong, Acta Crystallogr. 65 (2009) 66.
[18] G.M. Sheldrick, SHELXS-97, Program for Solution of Crystal Structures. University of Gottingen, Germany, 1997.
[19] A. Mann, A. Banso, L.C. Clifford, J. Tan., Health Res. 10 (2008) 34.
[20] B.S. Creaven, M. Devereux, D. Karcz, A. Kellett, M. McCann, A. Noble, M. Walsh, J. Inorg. Biochem. 103 (2009) 1196.
[21] I.R. Siddiqui, J. Singh, P.K. Singh, S. Dwivedi, P.K. Shukla, J. Singh, Indian J. Heterocycl. Chem. 14 (2005) 231.
[22] I.R. Siddiqui, J. Singh, P.K. Singh, J. Singh, Indian J. Chem. 44B (2005) 1460.
[23] I.R. Siddiqui, P.K. Singh, J. Singh, J. Singh, Indian J. Chem. 44B (2005) 2102.
[24] P.K. Singh, I.R. Siddiqui, Indian J. Chem. 48B (2009) 1013.
[25] I.R. Siddiqui, P.K. Singh, V. Srivastava, J. Singh, Indian J. Chem. 49B (2010) 512.